ISSN 2347-3487

Dielectric and Electrical Properties of LaGaO3 Ceramics

Anita Mekap, Piyush R. Das, *R. N. P. Choudhary

Department of Physics, Institute of Technical Education & Research,

Siksha 'O' Anusandhan University, Jagmohan Nagar,

Jagamara Bhubaneswar – 751030, India

E-mail: anitamekap@gmail.com , prdas63@gmail.com , crnpfl@gmail.com

Abstract

$LaGaO_3$ -based perovskite oxides doped with Sr and Mg exhibit high ionic conductivity over a wide range of oxygen partial pressure and found to be very stable in reducing, oxidizing, and CO_2 atmospheres. In this study, the polycrystalline sample of $LaGaO_3$ was prepared by a high-temperature solid-state reaction technique. Preliminary X-ray diffraction (XRD) studies of powder sample of $LaGaO_3$ showed the formation of single-phase compound at room temperature. The surface morphology of the pellet sample of $LaGaO_3$ was recorded at room temperature using a scanning electron microscope (SEM). Detailed studies of dielectric properties (ε_r, tan δ) and impedance parameters of the material provide an insight into the electrical properties and understanding of types of relaxation process occurred in the material. Temperature variation of dc conductivity shows that this compound exhibits negative temperature coefficient of resistance (NTCR) and frequency dependence of ac conductivity suggests that the material obeys Jonscher's universal power law.

Keywords: Ceramics; XRD; SEM; Electrical conductivity; Impedance spectroscopy.

*Corresponding author:

E-mail: crnpfl@gmail.com Ph- +918763425977, Fax-+91674-2351217

Council for Innovative Research

Peer Review Research Publishing System

Journal of Advances in Physics

Vol 3, No.2

editor@cirworld.com

www.cirworld.com, member.cirworld.com

ISSN 2347-3487

1. INTRODUCTION

Perovskite type oxides, AB_2O_3, have stable crystal structures, and furthermore, a large no of oxide vacancies can be introduced into the lattice by the partial substitution of cation A or B with lower valence cation. $LaGaO_3$- based perovskite oxides doped with Sr and Mg exhibit high ionic conductivity over a wide range of oxygen partial pressure [1]. The $LaGaO_3$-based oxide was found to be very stable in reducing, oxidizing, and CO_2 atmospheres. $LaGaO_3$ -based perovskite-type oxide can be used as electrolyte in intermediate-temperature Solid oxide fuel cells (SOFCs) [2]. Not much information on capacitive and conducting behavior of $LaGaO_3$ is available. Therefore, we have prepared and characterized $LaGaO_3$.The material has been extensively studied so that suitable substitutable doping can enhance its properties for different applications. In this paper, we report some important features of dielectric and electrical properties.

2. EXPERIMENTAL

Polycrystalline sample of $LaGaO_3$ was prepared from high purity raw materials, La_2O_3 (99%, M /s. Loba Chemie Pvt. Ltd., India) and Ga_2O_3 (99.9 %, M /s. Otto Chemie Pvt. Ltd., India) using a high-temperature solid-state reaction technique. These ingredients (taken in suitable stochiometry) were thoroughly mixed and ground in dry and wet (methanol) medium for 1 h each in an agate mortar. First, calcination was carried out in a high purity alumina crucible at 1150 ^{0}C for 12 h. The quality and formation of the compound were checked by an X-ray diffraction (XRD) technique. Room temperature (25^{0}C) XRD pattern of compound was obtained using an X-ray powder diffractometer (PHILIPS PW1817) with Cuk_α radiation (λ = 1.5418Á) in a wide range of Bragg angles ($20^0 \le 2\theta \le 80^0$) at a scanning rate of 3 deg. /min. The fine and homogeneous powder was then cold pressed into pellets (10 mm diameter and 1-2 mm thickness) under a uniaxial pressure of $5x10^6$ N/m^2 by a hydraulic press. Polyvinyl alcohol (PVA) was used as a binder during preparation of pellets. The pellets were then sintered for 10 h at 1150 ^{0}C in air atmosphere. The sintered pellets were then polished with fine emery paper in order to make both the faces flat and parallel. The pellets were then electroded with high purity air-drying silver paste, and then dried at 150^{0}C for 4 h, to remove moisture. The dielectric and electrical conductivity were studied on the sintered pellet of the compound, and the data were recorded using a computer-controlled phase sensitive meter (model N4L-PSM1795) (with a laboratory-made sample holder and a heating arrangement) over a wide range of temperature.

3. Results and Discussion

3.1 Structure/Microstructure

Fig. 1 shows the XRD pattern of calcined powder of the compound at room temperature. The sharp and single XRD peaks, which are different from that of ingredients, suggest formation of a single-phase new compound [3]. Generally, a good agreement between observed (obs.) and calculated (cal.) interplanar spacing (d) was found in orthorhombic crystal system and a selected unit cell. The selected lattice parameters (a, b and c) of a unit cell were refined using least-squares refinement sub-routine of POWD [4]. All of the diffraction peaks can be indexed to those of the lanthanum gallate ($LaGaO_3$) with lattice constants *a* = 6.6592 Å, b=5.4643 Å, *c* = 6.0668 Å and volume V=220.76 Å^3. Table 1 shows the correctness of the selection of crystal system and lattice parameters. Fig.2 shows the surface morphology of the pellet sample of $LaGaO_3$ recorded at room temperature using a scanning electron microscope (SEM). In spite of optimized sintering temperature, some voids of irregular shape and dimension are still observed. Small size grains are homogenously distributed throughout the surface of the sample.

3.2. Dielectric Study.

The temperature dependence of relative dielectric constant (ε_r) and dielectric loss (tan δ) at three different frequencies (11 kHz, 105 kHz, 500 kHz and 1 MHz) are shown in Fig. 3. The value of ε_r is almost constant at low temperatures but increases sharply at high temperature. The nature of variation of tan δ with temperature follows the similar pattern as of ε_r. The observed reduction of ε_r on increasing frequencies is a general characteristic of dielectric material. It has also been observed that tan δ changes very slowly with temperature up to 600 K, beyond that it increases very fast. The sharp increase in tan δ at higher temperatures may be due to scattering of thermally activated charge carriers and some defects in the sample [5]. At higher temperatures the conductivity begins to dominate, which in turn, is responsible for rise in tan δ.

3.3. Electrical Properties: Complex Impedance Spectroscopy

Complex impedance spectroscopy (CIS) is an important and powerful technique in studying the electrical properties such as contribution of bulk (grain), grain boundary and electrode polarization of the materials by different equivalent circuits. The complex impedance of the samples can be modeled as a parallel combination of RC (*R* = resistance and *C* = capacitance) circuits. The frequency dependence of electrical properties of a material is represented in terms of complex impedance. The frequency dependent properties of materials can be described via the complex dielectric permittivity (ε*), complex impedance (Z*), complex admittance (Y*), complex electric modulus (M*) and dielectric loss (tanδ).These parameters are related to each other by the following relations ;

$Z^*=Z' - jZ'' = 1/j\,\omega C_0\varepsilon$; $M^*=1/\varepsilon^*=M'+jM''=j\omega C_0 Z$; $Y^*=Y'+jY''=j\omega C_0\varepsilon^*$ and $\tan\delta = \varepsilon''/\varepsilon' = M'' / M' = Z'/Z'' = Y'/Y''$, where $\omega = 2\pi f$ is the angular frequency, C_0 is the geometrical capacitance, $j = \sqrt{-1}$).

Fig. 4 shows the temperature dependence of complex impedance spectra (Nyquist plot) of the said compound over a wide range of frequency. The ZSIMP WIN version 2.0) of software was used to analyzed the data. In an ideal case (Debye-like response), an equivalent circuit has parallel combination of CQR and CR where Q is known as constant phase element

(CPE), R is the resistance and C is the capacitance. Value of n is between zero and one (for an ideal capacitor n=1 and for an ideal resistor n=0) [6].

Using the fitted curves, the values of bulk resistance (R_b) and bulk capacitance (C_b) at different temperatures were calculated and compared in Table 2. The decreasing trend in the value of R_b on increasing temperature clearly indicates the existence of negative temperature co-efficient of resistance (NTCR) in the material as generally observed in semiconductors [7]. No grain boundary and interfacial effect were observed.

A perfect semi-circle with its center at Z'-axis is observed for an ideal Debye-type relaxation. However, in the studied material we did not get Debye-type of relaxation. Depressed semi-circles indicate the presence of non-Debye type of relaxation [8, 9]. The intercept of each semi-circle on real Z'-axis gives the contributions of bulk in the resistance/impedance. The semi-circles of the impedance spectra have characteristic peaks occurring at a unique relaxation frequency usually referred as relaxation frequency (f_r).

Fig.5 shows the variation of real and imaginary parts of impedance (i.e., Z' and Z") as a function of frequency at different temperature. The value of Z' decreases with rise in temperature and frequency. It suggests reduction in bulk resistance. It is also observed that the value of Z' decreases till a certain fixed frequency up to 100 kHz, and attain a constant value above this frequency implying the possible release of space charge [10]. Further, the frequency at which Z' becomes independent of frequency has been found to remain same with rise in temperature. This indicates the absence of frequency relaxation process in the material [6]. The value of Z" attains maxima at higher temperatures. The values of $Z"_{max}$ decrease with rise in temperature. This explains the presence of relaxation in the sample [11]. The broadening of $Z"_{max}$ peak with increase of temperature suggests the occurrence of temperature dependence of relaxation phenomenon in the material. The relaxation process occurs due to the presence of immobile charges at low temperatures and defects and vacancies at higher temperatures [12, 13].

3.4 ac Conductivity

Study of ac conductivity is carried out to understand the frequency dependence of electrical properties of the material. The frequency dependence of ac conductivity also provides information regarding the nature of charge carriers. The ac electrical conductivity (σ_{ac}) was calculated using the dielectric data in an empirical relation: $\sigma_{ac} = \omega\varepsilon_r\varepsilon_0 \tan\delta$, where ε_0 is permittivity in free space and ω is angular frequency. In order to have better understanding of conduction mechanism in the material, Jonscher's universal power law [14] is used: $\sigma_T(\omega) = \sigma(0) + \sigma_1(\omega) = \sigma_0 + a\omega^n$ where σ(0) is the frequency independent term giving dc conductivity and $\sigma_1(\omega)$ is the purely dispersive component of ac conductivity having a characteristic of power law behavior in terms of frequency (ω). The exponent n can have values in between 0 to 1. This parameter is frequency independent but temperature and material dependent.

Fig. 6 shows the variation of ac conductivity of the material as a function of frequency at different temperatures with non-linear fitting which referred as conductivity spectrum. The conductivity curves show dispersion in the low frequency region. From the graphs, it is obvious that σ_{ac} increases with rise in frequency but it is nearly independent at low frequency. The extrapolation of this part towards lower frequency side gives σ_{dc}. The increasing trend of σ_{ac} with rise in frequency in lower frequency region may be attributed to the disordering of cations between neighboring sites, and presence of space charge. In the high frequency region, the curves approach each other.

A close look on the conductivity plots reveals that the curves exhibit low frequency dispersion phenomena obeying the Jonscher's power law equation. According to Jonscher [12], the origin of the frequency dependence of conductivity lies in the relaxation phenomena arising due to mobile charge carriers. The conduction behavior of the materials obeys the power law; $\sigma(\omega) \alpha \omega^n$ with a slope change governed by n in the low temperature region. The value of n≤1 means that the hopping motion involves a translational motion with a sudden hopping whereas n>1 means that the motion involves localized hopping without the species leaving the neighborhood.. The low frequency dispersion has been attributed to the ac conductivity whereas the frequency independent plateau region corresponds to the dc conductivity. From non-linear fitting it is found that that motion of charge carriers is translational because of small value of n (< 1) [15]. The dc conductivity increases with rise in temperature (as expected) in the given material. The values of dc conductivity and n have been compared in Table.3.

Fig.7 shows the variation of σ_{ac} with temperature at selected frequencies. The ac conductivity was calculated using an empirical relation $\sigma_{ac} = \omega\varepsilon_r\varepsilon_o \tan\delta$ (ω = angular frequency, ε_o = vacuum permittivity). The value of σac decreases on decreasing temperature. The activation energy Ea (which is dependent on a thermally activated process) can be calculated using an empirical relation $\sigma_{ac} = \sigma_0 \exp(-Ea/kT)$ (k = Boltzmann constant, σ_0 = pre exponential factor). The value of ac conductivity clearly indicates that the conduction process of the material might be trap-controlled space-charge current conduction [16]. The value of E_a at temperature range (600-700K), calculated from the slope of the log σ_{ac} versus 1000/T plots for frequencies 11kHz, 105 kHz, 500 kHz and 1MHz was found to be 0.74, 0.51, 0.44 and 0.36eV respectively.

4. CONCLUSIONS

Finally, it is concluded that the titled compound $LaGaO_3$ has orthorhombic structure at room temperature. The dielectric constant as well as dielectric loss is almost constant at low temperature range. The compound is a low loss material. The contribution to the impedance comes from bulk only where the effect of grain boundary and interface is insignificant. This compound also exhibits negative temperature coefficient of resistance, which indicate the semi-conducting character of the material.

Acknowledgement

The authors are grateful to Dr. R. N. Maiti (CRF, IIT Kharagpur), Dr. Dilip Mishra of IMMT, Bhubaneswar and Samita Pattanaik of ITER for their help in experimental work and discussion.

References

1. Ishihara, T., Matsuda, H., Takita, Y. Doped $LaGaO_3$ Perovskite Type Oxide as a New Oxide Ionic Conductor. J. Am. Chem. Soc., 116 (1994) 3801-3803.
2. Ishihara, T., Honda, M., Shibayama, T., Minami, H., Nishiguchi, H., Takita, Y. Intermediate Temperature Solid Oxide Fuel Cells Using a New $LaGaO_3$ Based Oxide Ion Conductor: I. Doped $SmCoO_3$as a New Cathode Material. J. Electrochem. Soc. 145 (1998) 3177-3181.
3. H.P. Klug and L.E. Alexander, Wiley Chester (England) 1974, p966.
4. POWD E W, An Interactive Powder Diffraction Data Interpretation and Indexing

   Program, Version 2.1, School of Physical Science, Flinders University.
5. Ganguli, P., Devi, S., Jha, A.K., Deori, K.L. Dielectric and Pyroelectric Studies of Tungsten—Bronze Structured $Ba_5SmTi_3Nb_7O_{30}$ Ferroelectric Ceramics. Ferroelectrics 381(2009) 111.
6. Macdonald, J.R., Note on the parameterization of the constant-phase admittance element. Solid State Ionics 13 (1984) 147-149.
7. Ranjan, R., Kumar, R., Kumar, N., Behera, B., Choudhary, R. N. P., Impedance and electric modulus analysis of Sm-modified $Pb(Zr_{0.55}Ti_{0.45})_{1-x/4}O_3$ ceramics. J. Alloys. Comp. 509 (2011) 6388-6394.
8. Sen, S., Choudhary, R.N.P., Pramanik, P., Structural and electrical properties of Ca^{2+}-modified PZT electroceramics. Physica B 387(2007) 56-62.
9. Behera, B., Nayak, P., Choudhary, R.N.P., Impedance spectroscopy study of $NaBa_2V_5O_{15}$ ceramic. J. Alloys Compd. 436 (2007) 226-232.
10. Plcharski, J., Wieczoreck, W., PEO based composite solid electrolyte containing nasicon. Solid State Ionics 28-30 (1988) 979-982.
11. Behera, B., Nayak, P., Choudhary, R. N. P., Structural and impedance properties of $KBa_2V_5O_{15}$ ceramics. Mater. Res. Bull. 43 (2008) 401-410.
12. Jonscher, A.K., The 'universal' dielectric response. Nature 267(1977) 673-679.
13. Suman, C.K., Prasad, K., Choudhary, R.N.P., Complex impedance studies on tungsten-bronze electroceramic: $Pb_2Bi_3LaTi_5O_{18}$. J. Mater. Sci. 41 (2006) 369-375.
14. Sinclair, D. C., West, A. R., Impedance and modulus spectroscopy of semiconducting $BaTiO_3$ showing positive temperature coefficient of resistance. J. Appl. Phys. 66 (1989) 3850-3856.
15. Funke, K., Jump relaxation in solid electrolytes. Prog. Solid State Chem. 22 (1993) 111-195.
16. Pattanayak, S., Choudhary, R. N. P., Das, P.R., Effect of Gd-substitution on Phase transition and Conduction Mechanism of $BiFeO_3$. J. Mater. Sci: Mater Electron 24 (2013) 2767- 2771.

Figure captions

Fig.1. X-ray diffraction pattern of $LaGaO_3$

Fig.2. SEM micrograph of $LaGaO_3$ at room temperature

Fig.3. Variation of ε_r and (inset) tan δ with temperature at selected frequencies

Fig.4. Variation of Z' with Z'' at selected temperatures (Impedance fitting)

Fig.5. Variation of Z' &Z'' with frequency at selected temperatures

Fig.6. Variation of ac conductivity with frequency at selected temperatures

Fig.7. Variation of ac conductivity with temperature at selected frequencies

Table captions

Table.1. Comparison of d_{obs} , d_{cal} and hkl values of all reflection peaks of $LaGaO_3$

Table.2. Impedance fitting results of $LaGaO_3$

Table.3. Comparison of dc conductivity, ω and n at different temperatures of $LaGaO_3$

ISSN 2347-3487

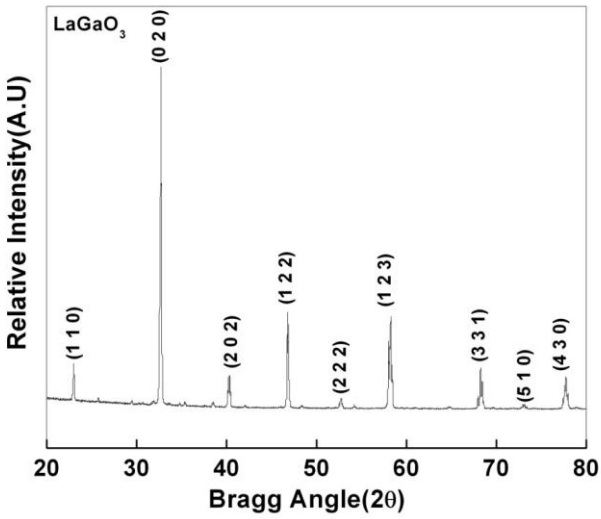

Fig.1. X-ray diffraction pattern of LaGaO3

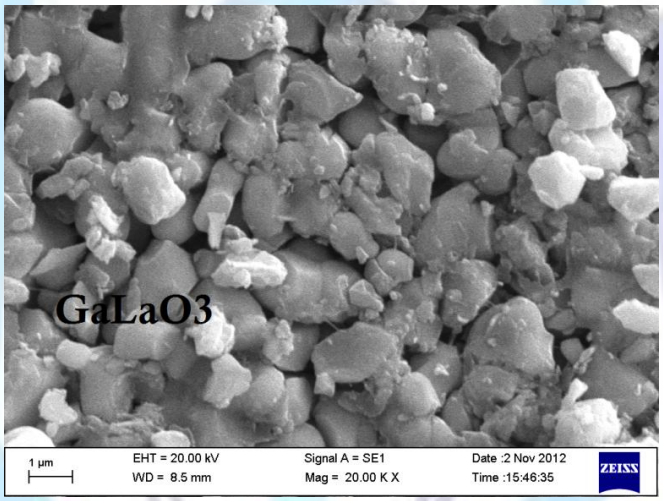

Fig.2. SEM micrograph of LaGaO3 at room temperature

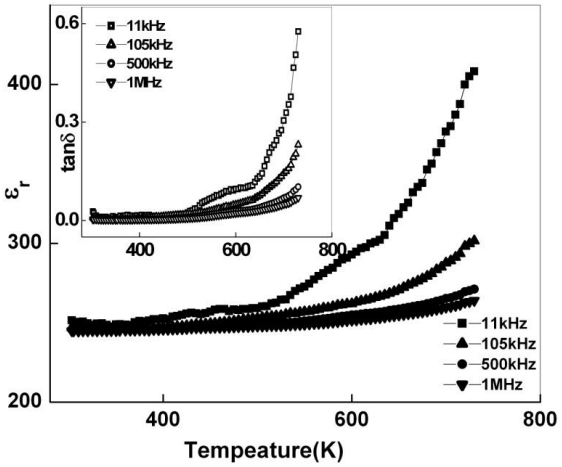

Fig.3. Variation of εr and (inset) tan δ with temperature at selected frequencies

ISSN 2347-3487

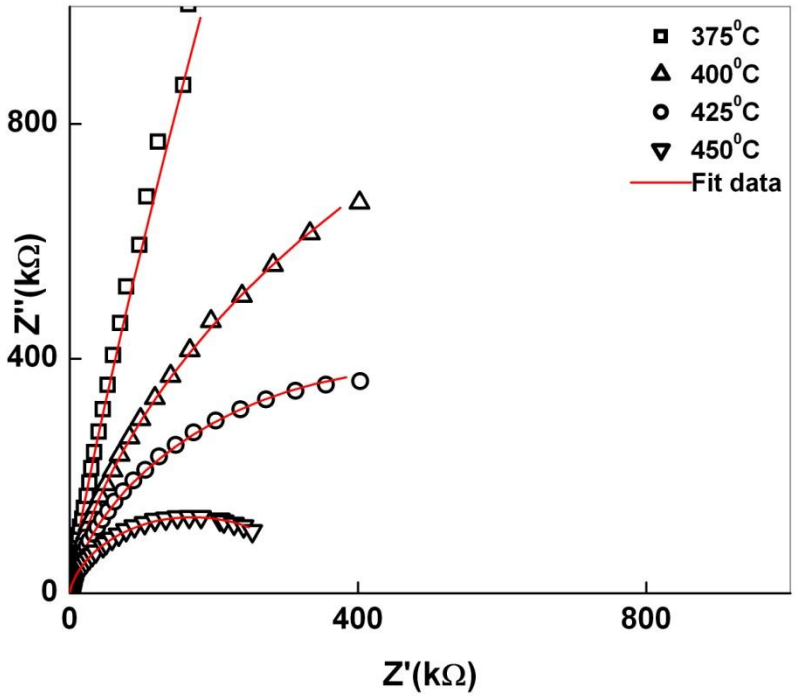

Fig.4. Variation of Z' with Z" at selected temperatures (Impedance fitting)

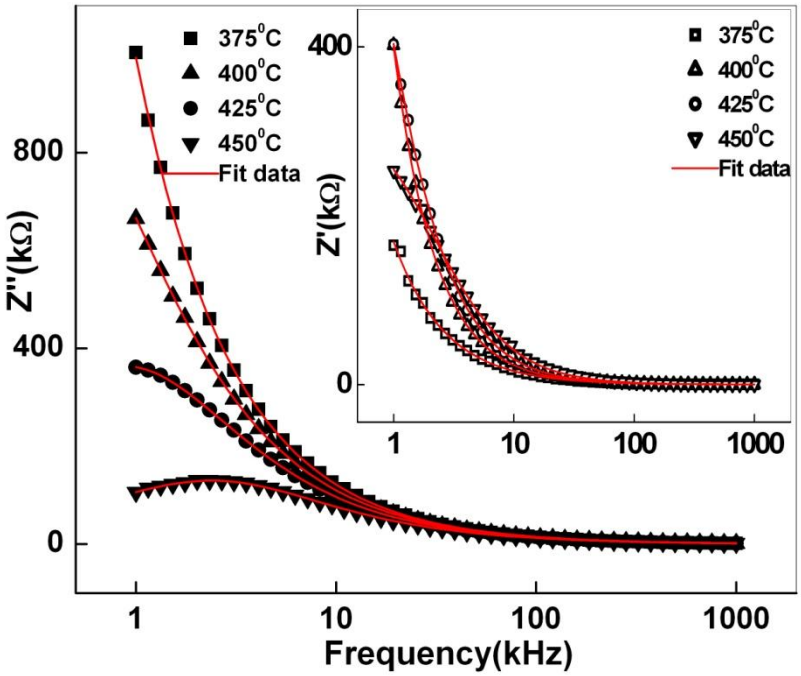

Fig.5. Variation of Z' & Z" with frequency at selected temperatures

ISSN 2347-3487

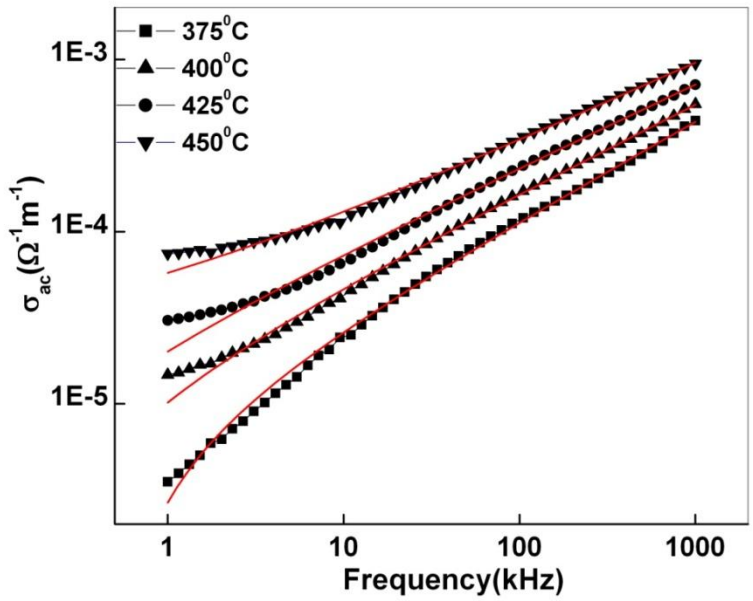

Fig.6. Variation of ac conductivity with frequency at selected temperatures

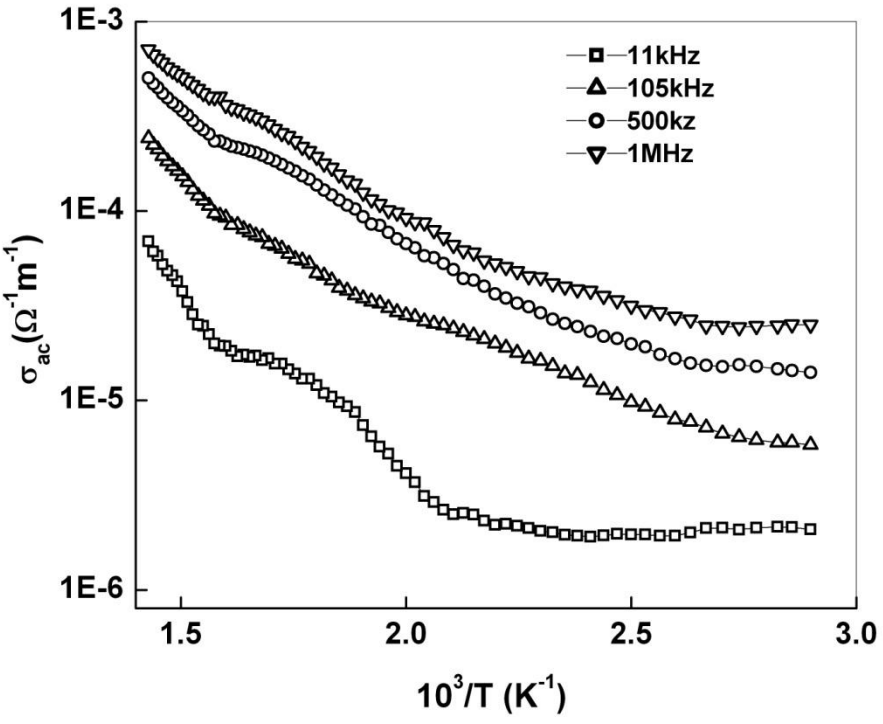

Fig.7. Variation of ac conductivity with temperature at selected frequencies

ISSN 2347-3487

Table.1. Comparison of dobs , dcal and hkl values of all reflection peaks of LaGaO3

Sl. No.	Miller Indices			d_{obs}	d_{cal}	I/Io
	h	k	l			
1	1	1	0	4.2247	4.2242	13
2	0	2	0	2.7313	2.7322	100
3	2	0	2	2.2419	2.2424	10
4	1	2	2	1.9406	1.9419	29
5	2	2	2	1.7329	1.7333	3.8
6	1	2	3	1.5811	1.5794	28
7	3	3	1	1.3725	1.3716	13
8	5	1	0	1.2942	1.2940	2.6
9	4	3	0	1.2282	1.2288	11

Table.2. Impedance fitting results of LaGaO3

T (^{0}C)	Rb(Ω)	Cb(F)	Q	n
375 ^{0}C	4.872×10^{13}	8.862×10^{-11}	6.930×10^{-10}	17.446
400^{0}C	2.922×10^{6}	9.109×10^{-11}	1.683×10^{-9}	6.819×10^{-1}
425^{0}C	1.042×10^{6}	8.805×10^{-11}	2.030×10^{-9}	6.901×10^{-1}
450 ^{0}C	3.571×10^{5}	8.669×10^{-11}	2.981×10^{-9}	6.768×10^{-1}

Table.3. Comparison of dc conductivity, ω and n at different temperatures of LaGaO3

T(^{o}C)	σ_{dc} (ohm^{-1}m^{-1})	ω	n
375	0 .000005	1.665×10^{-7}	0.57031
400	0.000012	4.6379×10^{-7}	0.5125
425	0.000015	9.3367×10^{-7}	0.48118
450	0.00002	1.5807×10^{-6}	0.46232